(12) INTERNATIONAL APPLICATION PUBLISHED UNDER THE PATENT COOPERATION TREATY (PCT)

(19) World Intellectual Property Organization
International Bureau

(43) International Publication Date
4 February 2010 (04.02.2010)

PCT

(10) International Publication Number
WO 2010/014215 A2

(51) International Patent Classification:
C01B 31/02 (2006.01) ***H01M 10/36*** (2010.01)
C01B 31/04 (2006.01) ***H01M 16/00*** (2006.01)
H01M 10/00 (2006.01) ***H01M 10/052*** (2010.01)

(21) International Application Number:
PCT/US2009/004369

(22) International Filing Date:
28 July 2009 (28.07.2009)

(25) Filing Language: English

(26) Publication Language: English

(30) Priority Data:
61/084,140 28 July 2008 (28.07.2008) US
12/460,993 27 July 2009 (27.07.2009) US

(71) Applicant *(for all designated States except US)*: **BATTELLE MEMORIAL INSTITUTE** [US/US]; Pacific Northwest Division, Intellectual Property Legal Services, P.O. Box 999, Richland, WA 99352 (US).

(71) Applicant *(for US only)*: **THE TRUSTEES OF PRINCETON UNIVERSITY** [US/US]; One Nassau Hall, Princeton, NJ 08544 (US).

(72) Inventors; and

(75) Inventors/Applicants *(for US only)*: **LIU, Jun** [US/US]; 2860 Hawkstone Court, Richland, WA 99334 (US). **AKSAY, Ilhan, A.** [US/US]; 16 Kimberly Court, Princeton, NJ 08540 (US). **CHOI, Daiwon** [KR/US]; 1409 Chardonnay Drive, Richland, WA 99352 (US). **WANG, Donghai** [CN/US]; 2455 George Washington Way, Richland, WA 99354 (US). **YANG, Zhenguo** [US/US]; 2926 Rock Creek Court, Richland, WA 99354 (US).

(74) Agents: **BRANTON, Vincent A.** et al.; Battelle Memorial Institute, P.O. Box 999 (MSIN K1-53), Richland, WA 99352 (US).

(81) Designated States *(unless otherwise indicated, for every kind of national protection available)*: AE, AG, AL, AM, AO, AT, AU, AZ, BA, BB, BG, BH, BR, BW, BY, BZ, CA, CH, CL, CN, CO, CR, CU, CZ, DE, DK, DM, DO, DZ, EC, EE, EG, ES, FI, GB, GD, GE, GH, GM, GT,

[Continued on next page]

(54) Title: NANOCOMPOSITE OF GRAPHENE AND METAL OXIDE MATERIALS

(57) Abstract: Nanocomposite materials comprising a metal oxide bonded to at least one graphene material. The nanocomposite materials exhibit a specific capacity of at least twice that of the metal oxide material without the graphene at a charge/discharge rate greater than about 10C.

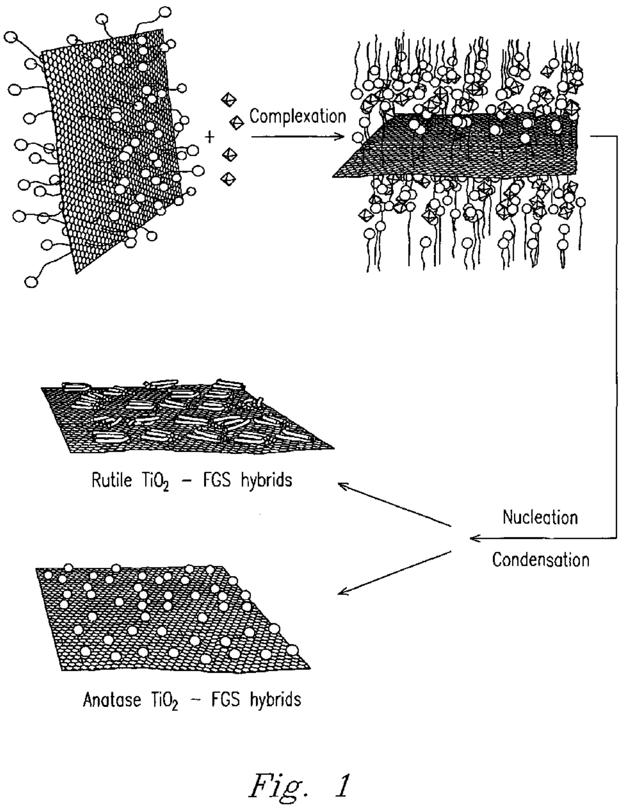

Fig. 1

WO 2010/014215 A2

HN, HR, HU, ID, IL, IN, IS, JP, KE, KG, KM, KN, KP, KR, KZ, LA, LC, LK, LR, LS, LT, LU, LY, MA, MD, ME, MG, MK, MN, MW, MX, MY, MZ, NA, NG, NI, NO, NZ, OM, PE, PG, PH, PL, PT, RO, RS, RU, SC, SD, SE, SG, SK, SL, SM, ST, SV, SY, TJ, TM, TN, TR, TT, TZ, UA, UG, US, UZ, VC, VN, ZA, ZM, ZW.

(84) **Designated States** *(unless otherwise indicated, for every kind of regional protection available)*: ARIPO (BW, GH, GM, KE, LS, MW, MZ, NA, SD, SL, SZ, TZ, UG, ZM, ZW), Eurasian (AM, AZ, BY, KG, KZ, MD, RU, TJ, TM), European (AT, BE, BG, CH, CY, CZ, DE, DK, EE, ES, FI, FR, GB, GR, HR, HU, IE, IS, IT, LT, LU, LV, MC, MK, MT, NL, NO, PL, PT, RO, SE, SI, SK, SM, TR), OAPI (BF, BJ, CF, CG, CI, CM, GA, GN, GQ, GW, ML, MR, NE, SN, TD, TG).

Published:

— *without international search report and to be republished upon receipt of that report (Rule 48.2(g))*

Nanocomposite of Graphene and Metal Oxide Materials

CROSS REFERENCE TO RELATED APPLICATIONS

[001] This application claims priority to US Provisional Application No. 61/084,140 filed July 28, 2008, entitled Metal Oxide-Graphene Hybrid Nanostructures and Method of Making and to the corresponding US Utility Application, entitled Nanocomposite of Graphene and Metal Oxide Materials filed July 27, 2009.

[002] The invention was made with Government support under Contract DE-AC0676RLO 1830, awarded by the U.S. Department of Energy. The Government has certain rights in the invention.

TECHNICAL FIELD

[003] This invention relates to nanocomposite materials of graphene bonded to metal oxides and methods for forming nanocomposite materials of graphene bonded to metal oxides.

BACKGROUND OF THE INVENTION

[004] Graphene is generally described as a one-atom-thick planar sheet of sp2-bonded carbon atoms that are densely packed in a honeycomb crystal lattice. The carbon-carbon bond length in graphene is approximately 0.142 nm. Graphene is the basic structural element of some carbon allotropes including graphite, carbon nanotubes and fullerenes. Graphene exhibits unique properties, such as very high strength and very high conductivity. Those having ordinary skill in the art recognize that many types of materials and devices may be improved if graphene is successfully incorporated into those materials and devices, thereby allowing them to take advantage of graphene's unique properties. Thus, those having ordinary skill in the art recognize the need for new methods of fabricating graphene and composite materials that incorporated graphene.

[005] Graphene has been produced by a variety of techniques. For example, graphene is produced by the chemical reduction of graphene oxide, as shown in Gomez-Navarro, C.; Weitz, R. T.; Bittner, A. M.; Scolari, M.; Mews, A.; Burghard, M.; Kern, K. Electronic Transport Properties of Individual Chemically Reduced Graphene Oxide Sheets. and *Nano Lett.* 2007, *7*, 3499-3503.Si, Y.; Samulski, E. T. Synthesis of Water Soluble Graphene. *Nano Lett.* 2008, *8*, 1679-1682.

[006] While the resultant product shown in the forgoing methods is generally described as graphene, it is clear from the specific capacity of these materials that complete reduction is not achieved, because the resultant materials do not approach the theoretical specific capacity of neat graphene. Accordingly, at least a portion of the graphene is not reduced, and the resultant material contains at least some graphene oxide. As used herein, the term "graphene" should be understood to encompass materials such as these, that contain both graphene and small amounts of graphene oxide.

[007] For example, functionalized graphene sheets (FGSs) prepared through the thermal expansion of graphite oxide as shown in McAllister, M. J.; LiO, J. L.; Adamson, D. H.; Schniepp, H. C.; Abdala, A. A.; Liu, J.; Herrera-Alonso, M.; Milius, D. L.; CarO, R.; Prud'homme, R. K.; Aksay, I. A. Single Sheet

Functionalized Graphene by Oxidation and Thermal Expansion of Graphite. *Chem. Mater.* 2007, *19*, 4396-4404 and Schniepp, H. C.; Li, J. L.; McAllister, M. J.; Sai, H.; Herrera-Alonso, M.; Adamson, D. H.; Prud'homme, R. K.; Car, R.; Saville, D. A.; Aksay, I. A. Functionalized Single Graphene Sheets Derived from Splitting Graphite Oxide. *J. Phys. Chem. B* 2006, *110*, 8535-8539 have been shown to have tunable C/O ratios ranging from 10 to 500. The term "graphene" as used herein should be understood to include both pure graphene and graphene with small amounts of graphene oxide, as is the case with these materials.

[008] Further, while graphene is generally described as a one-atom-thick planar sheet densely packed in a honeycomb crystal lattice, these one-atom-thick planar sheets are typically produced as part of an amalgamation of materials, often including materials with defects in the crystal lattice. For example, pentagonal and heptagonal cells constitute defects. If an isolated pentagonal cell is present, then the plane warps into a cone shape. Likewise, an isolated heptagon causes the sheet to become saddle-shaped. When producing graphene by known methods, these and other defects are typically present.

[009] The IUPAC compendium of technology states: "previously, descriptions such as graphite layers, carbon layers, or carbon sheets have been used for the term graphene...it is not correct to use for a single layer a term which includes the term graphite, which would imply a three-dimensional structure. The term graphene should be used only when the reactions, structural relations or other properties of individual layers are discussed". Accordingly, while it should be understood that while the terms "graphene" and "graphene layer" as used in the present invention refers only to materials that contain at least some individual layers of single layer sheets, the terms “graphene” and “graphene layer” as used herein should therefore be understood to also include materials where these single layer sheets are present as a part of materials that may additionally include graphite layers, carbon layers, and carbon sheets.

[0010] The unique electrical and mechanical properties of graphene have led to interest in its use in a variety of applications. For example, electrochemical energy storage has received great attention for potential applications in electric vehicles and renewable energy systems from intermittent wind and solar sources. Currently, Li-ion batteries are being considered as the leading candidates for hybrid, plug-in hybrid and all electrical vehicles, and possibly for utility applications as well. However, many potential electrode materials (e.g., oxide materials) in Li-ion batteries are limited by slow Li-ion diffusion, poor electron transport in electrodes, and increased resistance at the interface of electrode/electrolyte at high charging-discharging rates.

[0011] To improve the charge-discharge rate performance of Li-ion batteries, extensive work has focused on improving Li-ion and/or electron transport in electrodes. The use of nanostructures (e.g., nanoscale size or nanoporous structures) has been widely investigated to improve the Li-ion transport in electrodes by shortening Li-ion insertion/extraction pathway. In addition, a variety of approaches have also been developed to increase electron transport in the electrode materials, such as conductive coating (e.g., carbon), and uses of conductive additives (e.g., conductive oxide wires or networks, and conductive polymers). Recently, TiO_2 has been extensively studied to demonstrate the effectiveness of nanostructures and conductive coating in these devices.

[0012] TiO_2 is particularly interesting because it is an abundant, low cost, and environmentally benign material. TiO_2 is also structurally stable during Li-insertion/extraction and is intrinsically safe by avoiding Li electrochemical deposition. These properties make TiO_2 particularly attractive for large scale energy storage.

[0013] Another way to improve the Li-ion insertion properties is to introduce hybrid nanostructured electrodes that interconnect nanostructured electrode materials with conductive additive nanophases. For example, hybrid nanostructures, e.g., V_2O_5- carbon nanotube (CNT) or anatase TiO_2-CNT hybrids, $LiFePO_4$-RuO_2 nanocomposite, and anatase TiO_2-RuO_2 nanocomposite, combined with conventional carbon additives (e.g., Super P carbon or acetylene black) have demonstrated an increased Li-ion insertion/extraction capacity in the hybrid electrodes at high charge/discharge rates.

[0014] While the hybrids or nanocomposites offer significant advantages, some of the candidate materials to improve the specific capacity, such as RuO_2 and CNTs, are inherently expensive. In addition, conventional carbon additives at high loading content (e.g., 20 wt% or more) are still needed to ensure good electron transport in fabricated electrodes. To improve high-rate performance and reduce cost of the electrochemically active materials, it is important to identify high surface area, inexpensive and highly conductive nanostructured materials that can be integrated with electrochemical active materials at nanoscale.

[0015] Those having ordinary skill in the art recognize that graphene may be the ideal conductive additive for applications such as these hybrid nanostructured electrodes because of its high surface area (theoretical value of

2630 m^2/g), which promises improved interfacial contact, the potential for low manufacturing cost as compared to CNTs, and high specific capacity. Recently, high-surface-area graphene sheets were studied for direct Li-ion storage by expanding the layer spacing between the graphene sheets as described in Yoo, E.; Kim, J.; Hosono, E.; Zhou, H.-s.; Kudo, T.; Honma, I. Large Reversible Li Storage of Graphene Nanosheet Families for Use in Rechargeable Lithium Ion Batteries. *Nano Lett.* 2008, *8*, 2277-2282. In addition to these studies, graphene has also been used to form composite materials with SnO_2 for improving capacity and cyclic stability of the anode materials as described in Paek, S.-M.; Yoo, E.; Honma, I. Enhanced Cyclic Performance and Lithium Storage Capacity of SnO_2/Graphene Nanoporous Electrodes with Three-Dimensionally Delaminated Flexible Structure. *Nano Lett.* 2009, *9*, 72-75.

[0016] While these results were promising, they fell short of producing materials exhibiting specific capacity approaching the theoretical possibilities. For example, while it has been shown that graphene may be combined with certain metal oxides, the graphene materials in these studies fall far short of the theoretical maximum conductivity of single-sheet graphene. Further, those having ordinary skill in the art recognize that the carbon:oxygen ratio and the specific surface area of graphene provide an excellent proxy to measure the relative abundance of high conductivity single-sheets in a given sample. This is because the C:O ratio is a good measure of the degree of “surface functionalization” which affects conductivity, and the surface area conveys the percentage of single-sheet graphene in the synthesized powder.

[0017] Accordingly, those having ordinary skill in the art recognize that improvements to these methods are required to achieve the potential of using graphene nanostructures in these and other applications. Specifically, those skilled in the art recognize the need for new methods that produce nanocomposite materials of graphene and metal oxides that exhibit greater specific capacity than demonstrated in these prior art methods.

[0018] The present invention fulfills that need, and provides such improved composite nanostructures of graphene layers and metal oxides that exhibit specific capacities heretofore unknown in the prior art. The present invention further provides improved and novel methods for forming these composite nanostructures, and improved and novel devices that take advantage of the new and unique properties exhibited by these materials. The present invention meets these objectives by making nanostructures of graphene layers and metal oxides where the C:O ratio of the graphene layers in these nanostructures is between 15-500:1, and preferably 20-500:1, and the surface area of the graphene layers in these nanostructures is 400-2630 m2/g, and preferably 600-2630 m2/g, as measured by BET nitrogen adsorption at 77K. While those having ordinary skill in the art have recognized the desirability of having C:O ratios and surface areas this high in the graphene of nanostructures of graphene and metal oxides, the prior art methods have failed to produce them.

SUMMARY OF THE INVENTION

[0019] The present invention thus includes a nanocomposite material comprising a metal oxide bonded to at least one graphene layer. The metal oxide is preferably M_xO_y, and where M is selected from the group consisting of Ti, Sn, Ni, Mn, V, Si, Co and combinations thereof. The nanocomposite materials of the present invention are readily distinguished from the prior art because they exhibit a specific capacity of at least twice that of the metal oxide material without the graphene at a charge/discharge rate greater than about 10C.

[0020] For example, while not meant to be limiting, an example where titania is used as the metal oxide, the resulting nanocomposite material has a specific capacity at least twice that of a titania material without graphene at a charge/discharge rate greater than about 10C. Continuing the example, where titania is used as the metal oxide, the titania may be provided in a mesoporous form, and the mesoporous titania may further be provided in a rutile crystalline structure, or in an anatase crystalline structure.

[0021] The nanocomposite material of the present invention preferably is provided as graphene layers with metal oxides uniformly distributed throughout the nanoarchitecture of the layers. Preferably, but not meant to be limiting, the nanocomposite material of the present invention provides a metal oxide bonded to at least one graphene layer that has a thickness between 0.5 and 50 nm. More preferably, but also not meant to be liming, the nanocomposite material of the present invention provides a metal oxide bonded to at least one graphene layer that has a thickness between 2 and 10 nm. Preferably, the carbon to oxygen ratio (C:O) of the graphene in the nanostructures of the present invention is between 15-500:1, and more preferably between 20-500:1. Preferably, the surface area of the graphene in the nanostructures of the present invention is between 400-2630 m2/g, and more preferably between 600-2630 m2/g, as measured by BET nitrogen adsorption at 77K.

[0022] Another aspect of the present invention is a method for forming the nanocomposite materials of graphene bonded to metal oxide. The method consists of the steps of providing graphene in a first suspension; dispersing the graphene with a surfactant; adding a metal oxide precursor to the dispersed graphene to form a second suspension; and precipitating the metal oxide from the second suspension onto at least one surface of the dispersed graphene. In this manner, a nanocomposite material of at least one metal oxide bonded to at least one graphene layer is thereby formed. The nanocomposite materials formed in this manner are readily distinguished from materials formed by prior art methods because they exhibit a specific capacity of at least twice that of the metal oxide material without the graphene at a charge/discharge rate greater than about 10C.

[0023] Preferably, but not meant to be limiting, the first suspension is, at least in part, an aqueous suspension and the surfactant is an anionic surfactant. Also not meant to be limiting, a preferred anionic sulfate surfactant is sodium dodecyl sulfate. The method of the present invention may further comprise the step of heating the second suspension from 50 to 500 degrees C to condense the metal oxide on the graphene surface. The method of the present invention may also further comprise the step of heating the second suspension from 50 to 500 degrees C to remove the surfactant.

[0024] The present invention also encompasses an energy storage device comprising a nanocomposite material having an active metal oxide compound and one graphene layer arranged in a nanoarchitecture. The energy storage devices of the present invention are readily distinguished from prior art energy storage devices because they exhibit a specific capacity of at least twice that of the metal oxide material without the graphene at a charge/discharge rate greater than about 10C.

[0025] For example, while not meant to be limiting, an example where titania is used as the metal oxide, the energy storage device of the present invention has a specific capacity at least twice that of a titania material without graphene at a charge/discharge rate greater than about 10C.

[0026] Preferably, but not meant to be limiting, the energy storage device of the present invention is provided as having at least one component having a nanocomposite material having graphene layers with metal oxides uniformly distributed throughout the nanoarchitecture of the layers. Also preferably, but not meant to be limiting, the energy storage device of the present invention is an electrochemical device having an anode, a cathode, an electrolyte, and a current collector, wherein at least one of the anode, cathode, electrolyte, and current collector is fabricated, at least in part, from a nanocomposite material having graphene layers with metal oxides uniformly distributed throughout the nanoarchitecture of the layers.

[0027] In embodiments where the energy storage device of the present invention includes a cathode fabricated, at least in part, from a nanocomposite material having graphene layers with metal oxides uniformly distributed throughout the nanoarchitecture of the layers, the graphene in the cathode is preferably, but not meant to be limiting, 5% or less of the total weight of the cathode, and more preferably, but also not meant to be limiting, 2.5% or less of the total weight of the cathode. In this manner, the energy storage devices of the present invention are distinguished from prior art devices which are characterized by having more than 5% of the total weight of the cathode as carbon with no graphene.

[0028] In embodiments where the energy storage device of the present invention includes an anode fabricated, at least in part, from a nanocomposite material having graphene layers with metal oxides uniformly distributed throughout the nanoarchitecture of the layers, the graphene in the anode is preferably, but not meant to be limiting, 10% or less of the total weight of anode, and more preferably, but also not meant to be limiting, 5% or less of the total weight of anode. In this manner, the energy storage devices of the present invention are distinguished from prior art devices which are characterized by having more than 10% of the total weight of the anode as carbon with no graphene.

[0029] One embodiment where the present invention is an energy storage device is as a lithium ion battery. In this embodiment, the lithium ion battery has at least one electrode with at least one graphene layer bonded to titania to form a nanocomposite material, and the nanocomposite material has a specific capacity at least twice that of a titania material without graphene at a charge/discharge rate greater than about 10C. The electrode of this lithium ion battery may further have multiple nanocomposite material layers uniformly distributed throughout the electrode.

BRIEF DESCRIPTION OF THE DRAWINGS

[0030] The following detailed description of the embodiments of the invention will be more readily understood when taken in conjunction with the following drawing, wherein:

[0031] **Figure 1** is a schematic illustration of the present invention showing anionic sulfate surfactant mediated stabilization of graphene and growth of TiO_2-FGS hybrid nanostructures.

[0032] **Figure 2** is a graph showing high energy resolution photoemission spectra of the C 1s region in functionalized graphene sheets (FGS) used in one embodiment of the present invention.

[0033] **Figure 3** are Raman spectra of rutile TiO_2-FGS and FGS in one embodiment of the present invention.

[0034] **Figure 4(a)** is a photograph of FGS (left) and SDS-FGS aqueous dispersions (right); **Figure 4(b)** is a graph of the UV-Vis absorbance of the SDS-FGS aqueous dispersion.

[0035] **Figure 5** is an XRD pattern of one embodiment of the present invention, an anatase TiO_2-FGS and rutile TiO_2-FGS hybrid material. Standard diffraction peaks of anatase TiO_2 (JCPDS No. 21-1272) and rutile TiO_2 (JCPDS No. 21-1276) are shown as vertical bars.

[0036] **Figure 6(a)-(g)** are TEM and SEM images of the nanocomposite materials of various embodiments of the present invention at selected magnifications.

[0037] **Figure 7(a)-(f)** are graphs showing the electrical performance of one embodiment of the present invention. **Figure 7(a)** shows the voltage profiles for control rutile TiO_2 and rutile TiO_2-FGS (0.5 wt% FGS) hybrid nanostructures at C/5 charge-discharge rates. **Figure 7(b)** shows the specific capacity of control rutile TiO_2 and the rutile TiO_2-FGS hybrids at different charge/discharge rates; **Figure 7(c)** shows the cycling performance of the rutile TiO_2-FGS up to 100 cycles at 1C charge/discharge rates after testing at various rates shown in

Figure 7(b). **Figure 7(d)** shows the voltage profiles for control anatase TiO_2 and anatase TiO_2-FGS (2.5 wt% FGS) hybrid nanostructures at C/5 charge-discharge rates. **Figure 7(e)** shows the specific capacity of control anatase TiO_2 and the anatase TiO_2-FGS hybrids at different charge/discharge rates; **Figure 7(f)** shows the cycling performance of the anatase TiO_2-FGS up to 100 cycles at 1C charge/discharge rates after testing at various rates shown in **Figure 7(e)**.

[0038] **Figure 8** is a graph showing a plot of coulombic efficiency versus cycle number of TiO_2-FGS hybrids of one embodiment of the present invention at various charge/discharge rate between 1~3 V vs. Li/Li^+.

[0039] **Figure 9** is a graph showing the capacity of functionalized graphene sheets of one embodiment of the present invention as function of cycling numbers between 1~3 V vs. Li/Li^+.

[0040] **Figure 10(a)** is a graph showing the impedance measurement of coin cells using the electrode materials of control rutile TiO_2 and rutile TiO_2-FGS hybrids with different weight percentage of FGSs. **Figure 10(b)** is a graph showing the specific capacity of rutile TiO_2-CNT and rutile TiO_2-FGS at 30C rate with different percentages of graphene.

[0041] **Figure 11** is a graph showing the specific capacity of control rutile TiO_2 (10 wt% Super P) and rutile TiO_2-FGS hybrids (10 wt% FGS) at different charge/discharge rates. The rutile TiO_2-FGS hybrid electrode was prepared by mixing the calcined hybrid with PVDF binder at a mass ratio of 90:10. The control TiO_2 electrode was prepared by mixing control TiO_2 powder, Super P and PVDF binder at a mass ratio of 80:10:10.

[0042] **Figure 12** is an SEM image of TiO_2/FGS hybrid materials made in one embodiment of the present invention without using SDS as a stabilizer. As shown, TiO_2 and FGS domains are separated from each other with minor TiO_2 coated on FGS.

DETAILED DESCRIPTION OF THE PREFERRED EMBODIMENTS

[0043] For the purposes of promoting an understanding of the principles of the invention, reference will now be made to the embodiments illustrated in the drawings and specific language will be used to describe the same. It will nevertheless be understood that no limitations of the inventive scope is thereby intended, as the scope of this invention should be evaluated with reference to the claims appended hereto. Alterations and further modifications in the illustrated devices, and such further applications of the principles of the invention as illustrated herein are contemplated as would normally occur to one skilled in the art to which the invention relates.

[0044] A series of experiments were conducted to demonstrate certain embodiments of the present invention. In these experiments, anionic sulfate surfactants were used to assist the stabilization of graphene in aqueous solutions and facilitate the self-assembly of in-situ grown nanocrystalline TiO_2, rutile and anatase, with graphene. These nanostructured TiO_2-graphene hybrid materials were then used for investigation of Li-ion insertion properties. The hybrid materials showed significantly enhanced Li-ion insertion/extraction in TiO_2. The specific capacity was more than doubled at high charge rates, as compared with the pure TiO_2 phase. The improved capacity at high charge-discharge rate may be attributed to increased electrode conductivity in the presence of a percolated graphene network embedded into the metal oxide electrodes. While not to be limiting, these are among the features that distinguish the methods, materials, and devices of the present invention from the prior art.

[0045] These experiments thereby demonstrated that the use of graphene as a conductive additive in self-assembled hybrid nanostructures enhances high rate performance of electrochemical active materials. While the metal oxide TiO_2 was selected as a model electrochemical active oxide material, the method of the present invention is equally applicable to all metal oxides.

[0046] These experiments utilized a one-step synthesis approach to prepare metal oxide-graphene hybrid nanostructures. In these experiments, the reduced and highly conductive form of graphene is hydrophobic and oxides are hydrophilic. The present invention's use of surfactants not only solved the hydrophobic/hydrophilic incompatibility problem, but also provides a molecular template for controlled nucleation and growth of the nanostructured inorganics, resulting in a uniform coating of the metal oxide on the graphene surfaces.

[0047] This approach, schematically illustrated in Figure 1, starts with the dispersion of the graphene layers with an anionic sulfate surfactant. For example, but not meant to be limiting, sodium dodecyl sulfate. The method then proceeds with the self-assembly of surfactants with the metal oxide precursor and the *in-situ* precipitation of metal oxide precursors to produce the desired oxide phase and morphology.

[0048] In a typical preparation of rutile TiO_2-FGS hybrid materials (e.g., 0.5 wt% FGS), 2.4 mg FGSs and 3 mL SDS aqueous solution (0.5 mol/L) were mixed together. The mixture was diluted to 15 mL and sonicated for 10-15 min using a BRANSON SONIFER S-450A, 400W. 25 mL $TiCl_3$ (0.12 mol/L) aqueous solution was then added into as-prepared SDS-FGS dispersions while stirring. Then, 2.5 mL H_2O_2 (1 wt%) was added dropwise followed by de-ionized water under vigorous stirring until reaching a total volume of 80 mL. In a similar manner, 0.8, 26.4, and 60 mg FGSs were used to prepare the hybrid materials with 0.17, 5, and 10 wt% FGS, respectively.

[0049] Rutile TiO_2-CNT (0.5 wt% carbon nanotubes) hybrid materials were also prepared using corresponding single-wall CNTs (2.4 mg) according to the above method.

[0050] In a typical preparation of anatase TiO_2-FGS hybrid materials (e.g., 2.5 wt% FGS), 13 mg FGS and 0.6 mL SDS aqueous solution (0.5 mol/L) were mixed and sonicated to prepare an SDS-FGS dispersion. 25 mL $TiCl_3$ (0.12 mol/L) aqueous solution was added into as-prepared SDS-FGS dispersions while stirring followed by the addition of 5 mL 0.6 M Na_2SO_4. 2.5 mL H_2O_2 (1 wt%) was then added dropwise followed by addition of de-ionized water under vigorous stirring until reaching a total volume of 80 mL.

[0051] All of these resulting mixtures were further stirred in a sealed polypropylene flask at 90 °C for 16 h. The precipitates were separated by centrifuge followed by washing with de-ionized water and ethanol. The centrifuging and washing processes were repeated 3 times. The product was then dried in a vacuum oven at 70 °C overnight and subsequently calcined in static air at 400 °C for 2 h.

[0052] The thermal gravimetric analysis (TGA) indicated approximately 50 wt% percentage loss of FGSs during calcination in air at 400 °C for 2 h. The weight percentage of the graphene in the hybrid materials was thus correspondingly normalized, which is consistent with TGA of the hybrid materials.

[0053] The samples were characterized by XRD patterns obtained on a Philips Xpert X-ray diffractometer using Cu K_α radiation at $\lambda = 1.54$ Å. The TEM imaging was performed on a JEOL JSM-2010 TEM operated at 200 kV. SEM images were obtained on an FEI Helios Nanolab dual-beam focused ion beam/scanning electron microscope (FIB/SEM) operated at 2 kV. XPS characterization was performed using a Physical Electronics Quantum 2000 Scanning ESCA Microprobe with a focused monochromatic Al K_α X-ray (1486.7 eV) source and a spherical section analyzer. Electrochemical experiments were performed with coin cells (Type 2335, half-cell) using Li foil as counter electrode. The working electrode was prepared using the mixture of calcined TiO_2-FGS or control TiO_2, Super P and poly (vinylidene fluoride) (PVDF) binder dispersed in N–methylpyrrolidone (NMP) solution. For the preparation of rutile TiO_2 electrode (less than 5 wt% graphene), the mass ratio of rutile TiO_2-hybrid or control rutile TiO_2, Super P and PVDF was 80:10:10. For the preparation of anatase TiO_2 electrode, the mass ratio was 70:20:10 and 80:10:10 for control anatase TiO_2 and anatase TiO_2-FGS hybrid (2.5 wt% FGS), respectively.

[0054] Rutile TiO_2-FGS hybrid (10 wt% FGS) electrode was prepared with a mass ratio of hybrid and PVDF binder at 90:10 without Super P. The resultant slurry was then uniformly coated on an aluminum foil current collector and dried overnight in air. The electrolyte used was 1 M $LiPF_6$ dissolved in a mixture of ethyl carbonate (EC) and dimethyl carbonate (DMC) with the volume ratio of 1:1. The coin cells were assembled in an argon-filled glove box. The electrochemical performance of TiO_2-graphene was characterized with an Arbin Battery Testing System at room temperature. The electrochemical tests were performed between 3~1 V vs. Li^+/Li and C-rate currents applied were calculated based on a rutile TiO_2 theoretical capacity of 168 mAh/g.

[0055] Functionalized graphene sheets (FGSs) used in this study were prepared through the thermal expansion of graphite oxide according to the method shown in McAllister, M. J.; LiO, J. L.; Adamson, D. H.; Schniepp, H. C.; Abdala, A. A.; Liu, J.; Herrera-Alonso, M.; Milius, D. L.; CarO, R.; Prud'homme, R. K.; Aksay, I. A. Single Sheet Functionalized Graphene by Oxidation and Thermal Expansion of Graphite. *Chem. Mater.* **2007**, *19*, 4396-4404 and Schniepp, H. C.; Li, J. L.; McAllister, M. J.; Sai, H.; Herrera-Alonso, M.; Adamson, D. H.; Prud'homme, R. K.; Car, R.; Saville, D. A.; Aksay, I. A. Functionalized Single Graphene Sheets Derived from Splitting Graphite Oxide. *J. Phys. Chem. B* **2006**, *110*, 8535-8539. As discussed previously, in comparison to the graphene produced by the chemical reduction of graphene oxide, graphene prepared by the thermal expansion approach can have tunable C/O ratios ranging from 10 to 500 and thus its conductivity can be tuned to higher values.

[0056] FGSs processing starts with chemical oxidation of graphite flakes to increase the c-axis spacing from 0.34 to 0.7 nm. The resultant graphite oxide is then split by a rapid thermal expansion to yield separated graphene sheets. X-ray photoemission spectroscopy (XPS) of FGSs shows a sharp C1s peak indicating good sp^2 conjugation as shown in Figure 2. A small shoulder at 286 eV indicates the existence of some C-O bonds corresponding to the epoxy and hydroxyl functional groups on FGSs.

[0057] Sodium dodecyl sulfate (SDS)-FGS aqueous dispersions were prepared by ultrasonication. Similar to the colloidal stabilization of CNTs using SDS shown in Bonard, J. M.; Stora, T.; Salvetat, J. P.; Maier, F.; Stockli, T.; Duschl, C.; Forro, L.; deHeer, W. A.; Chatelain, A. Purification and Size-

Selection of Carbon Nanotubes. *Adv. Mater.* 1997, *9*, 827-831 and Richard, C.; Balavoine, F.; Schultz, P.; Ebbesen, T. W.; Mioskowski, C. Supramolecular Self-Assembly of Lipid Derivatives on Carbon Nanotubes. *Science* 2003, *300*, 775-778, the SDS-FGS aqueous dispersions were stable. Only minor sedimentation was observed after a week at room temperature as shown in Figure 4a.

[0058] UV-Vis spectrum of the SDS-FGS dispersion showed an absorption peak at 275 nm with a broad absorption background (Figure 4b) consistent with that of aqueous stable graphene sheets. Raman spectra of FGS and calcined TiO_2-FGS showed similar G and D bands structure of carbon, indicating that the structure of graphene is maintained during the synthesis procedure, as shown in Figure 3.

[0059] A mild, low-temperature (below 100 °C) crystallization process was carried out to form crystalline TiO_2 with controlled crystalline phase (i.e., rutile and anatase) on the graphene sheets. The low temperature condition was also important in preventing aggregation of graphene sheets at elevated temperatures. Consistent with previous studies, by the low-temperature oxidative hydrolysis and crystallization, rutile TiO_2-FGS is obtained with a minor anatase phase. To obtain anatase TiO_2-FGS, additional sodium sulfate was added to the solution to promote the formation of the anatase phase. XRD patterns of the TiO_2-FGS hybrids shown in Figure 5 show the formation of nanocrystalline rutile and anatase metal oxides with an estimated crystalline domain size of 6 and 5 nm, respectively.

[0060] Typical morphology of FGSs is shown in the transmission electron microscopy (TEM) image of Figure 6a. The free standing 2D FGSs are not perfectly flat but display intrinsic microscopic roughening and out-of-plane deformations (wrinkles). More than 80% of the FGSs have been shown to be single sheets by AFM characterization, when they were deposited onto an atomically smooth, highly oriented pyrolytic carbon (HOPG) template. Some regions appeared as multilayers in the TEM images, which may represent the regions that either have not been fully exfoliated or the regions that have restacked together due to capillary and van der Waals forces experienced during the drying process.

[0061] Figures 6b to 6e show TEM and scanning electron microscopy (SEM) images of as-grown rutile TiO_2-FGS hybrid nanostructures. Figures 6b and 6c show planar views of FGSs covered with nanostructured TiO_2. Both the edge of graphene and the nanostructure of the TiO_2 are clearly observable in the higher magnification image of Figure 6c.

[0062] The nanostructured TiO_2 is composed of rod-like rutile nanocrystals organized in parallel interspaced with the SDS surfactants. The SEM image of Figure 6d shows randomly oriented rod-like nanostructured rutile lying on the FGS. The cross-section TEM image further confirms that the nanostructured rutile mostly lies on the FGS with the rod length parallel to the graphene surface (Figure 6e). Figures 6f and 6g show plane-view TEM images of anatase TiO_2-FGS hybrid nanostructures. FGSs underneath are covered with spherical aggregated anatase TiO_2 nanoparticles. The dark field TEM image (Figure 6g) further confirms crystalline TiO_2 nanoparticles (bright regions) with a diameter of 5 nm spreading over the graphene surface.

[0063] It is important to note that the SDS surfactant determines the interfacial interactions between graphene and the oxide materials in promoting the formation of TiO_2-hybrid nanostructures. When the surfactant molecules are added, they can adsorb onto graphene through the hydrophobic tails making FGSs highly dispersed and interact with the oxide precursor through the hydrophilic head groups. The cooperative interactions between the surfactant, the graphene, and the oxide precursors lead to the homogeneous mixing of the components, in which the hydrophobic graphene most likely resides in the hydrophobic domains of the SDS micelles. As nanocrystalline TiO_2 formed, as-grown nanoparticles are then coated to the graphene surfaces since sulfate head groups have strong bonding with TiO_2. Without the surfactant, some of the surface functional sites (e.g., carboxylate, epoxy, and hydroxyl groups) on FGSs may provide bonding to TiO_2 nanoparticles. However, only a very small amount of the metal oxides will then be attached to graphene through such interactions due to the low number density of these functional groups on FGSs. Thus, in the control samples without the surfactant, FGSs are barely covered with the metal oxides along with phase separation from TiO_2 as shown in Figure 12. This indicates the important role of SDS in the formation of the self-assembled hybrid nanostructures.

[0064] To examine the effectiveness of FGSs in improving the rate capability of the electrode, we investigated the Li-ion insertion/extraction properties in the TiO_2-FGS hybrid materials. The electrodes were fabricated in a conventional way by mixing the hybrid materials with Super P carbon additive and a PVDF binder and thus tested in Li-ion battery coin cell. The rutile TiO_2-FGS hybrid showed a slope profile of voltage-capacity relationship at both the charge and discharge state as shown in Figure 7a, similar to that of control rutile TiO_2 and nanostructured rutile studied previously as reported in Hu, Y. S.; Kienle, L.; Guo, Y. G.; Maier, J. High Lithium Electroactivity of Nanometer-Sized Rutile TiO_2. *Adv.*

Mater. **2006**, *18*, 1421-1426. As shown in Figure 7b, with the incorporation of FGSs, the specific capacity of rutile TiO_2 in the hybrids (0.5 wt% FGS) increased at all charge/discharge rates compared with the control rutile TiO_2. The relative increase in specific capacity is especially larger at higher rates. For instance, at a rate of 30C (2 min of charging or discharging), the specific capacity of the rutile TiO_2-FGS hybrid material is 87 mAh/g which is more than double the high rate capacity (35 mAh/g) of the control rutile TiO_2 as shown in Figure 7b.

[0065] The voltage-capacity profile of anatase TiO_2-FGS (2.5 wt % FGS) at C/5 rate shows plateaus around 1.8 V (discharge process) and 1.9 V (charge process) is shown in Figure 7d, which is similar to that of control anatase TiO_2 and nanostructured anatase. The plateaus are related to the phase transition between the tetragonal and orthorhombic phases with Li insertion into anatase TiO_2. Similar to rutile TiO_2-FGS, the specific capacity of the anatase TiO_2-FGS hybrid is enhanced at all charge-discharge rates as shown in Figure 7e. The specific capacity of the anatase TiO_2-FGS at the rate of 30C is as high as 96 mAh/g compared with 25 mAh/g of control anatase TiO_2. Furthermore, the coulombic efficiencies of TiO_2-FGS hybrids at various charge/discharge rates are greater than 98% as shown in Figure 8. Both rutile and anatase TiO_2-FGS hybrids show good capacity retention of the Li-ion insertion/extraction with over 90% capacity retention after 100 cycles at a 1C rate, as shown in Figure 7c and 7f.

[0066] To identify the capacity contribution from FGSs, the Li-ion insertion/extraction behavior of the FGSs was also studied. The initial capacity of FGS of 100 mAh/g with 50% irreversible loss is observed between 1~3 V potential window applied, which is consistent with a recent study of Li-ion storage in graphene described in Yoo, E.; Kim, J.; Hosono, E.; Zhou, H.-s.; Kudo, T.; Honma, I. Large Reversible Li Storage of Graphene Nanosheet Families for Use in Rechargeable Lithium Ion Batteries. *Nano Lett.* **2008**, *8*, 2277-2282. However, the specific capacity of FGS rapidly decreases to 25 mAh/g within 10 cycles. At higher charge/discharge rates, FGS has almost negligible Li-ion insertion as shown in Figure 9. For 1 wt% FGS hybrids, the capacity contribution from FGS itself after 2 cycles can be a maximum value of 0.4 mAh/g. Thus, the increase of the specific capacity at high rate is not attributed to the capacity of the graphene additive itself in the hybrid materials.

[0067] To further understand the improved high-rate performance, electrochemical impedance spectroscopy measurements on rutile TiO_2-FGS hybrid materials were performed after cycles. The Nyquist plots of the rutile TiO_2-FGS electrode materials with different percentage of graphene cycled in electrolyte, as shown in Figure 10(a), all show depressed semicycles at high frequencies. As electrolyte and electrode fabrication are similar between each electrode, the high frequency semicircle should relate to the internal resistance of the electrode. We estimate that the resistivity of the cells decreased from 93 Ω for the pure TiO_2 to 73 Ω with the addition of only 0.5 wt% graphene.

[0068] By increasing the graphene percentage in the hybrid materials further, the specific capacity is slightly increased, e.g., to 93 mAh/g in the hybrid material with 5 wt% FGS, indicating that a kinetic capacity limitation may be reached by only improving the electrode conductivity with the incorporation of FGSs as shown in Figure 10(b). Rutile TiO_2-CNT hybrids prepared and tested under similar conditions showed poorer performance at identical carbon loadings than the rutile TiO_2-FGS hybrid anodes, as shown in the yellow bar in Figure 10(b).

Similarly, hybrid nanostructures prepared using solution reduced graphene oxides also showed even poorer performance, indicating the importance of the highly conductive graphene phase of FGSs.

[0069] To study the properties of electrode materials without any Super P carbon, Li-ion insertion/extraction properties of the rutile TiO_2-FGS (10 wt % graphene) were compared with control rutile TiO_2 with 10 wt% Super P at high charge-discharge rates. The hybrid material showed a much higher capacity at all charge-discharge rate, as shown in Figure 11. This result indeed confirms that the graphene in the self-assembled hybrid materials is more effective than the commonly used Super P carbon materials in improving high rate performance of the electrode materials.

[0070] The high rate performance is important for applications where fast charge and discharge is needed, such as in load leveling utility applications. The simple self-assembly approach, and the potential low manufacturing cost of graphene of the present invention, thus provide a new pathway for large scale applications of novel hybrid nanocomposite materials for energy storage.

[0071] While the invention has been illustrated and described in detail in the drawings and foregoing description, the same is to be considered as illustrative and not restrictive in character. Only certain embodiments have been shown and described, and all changes, equivalents, and modifications that come within the spirit of the invention described herein are desired to be protected. Any experiments, experimental examples, or experimental results provided herein are intended to be illustrative of the present invention and should not be considered limiting or restrictive with regard to the invention scope. Further, any theory, mechanism of operation, proof, or finding stated herein is meant to further enhance understanding of the present invention and is not intended to limit the present invention in any way to such theory, mechanism of operation, proof, or finding.

[0072] Thus, the specifics of this description and the attached drawings should not be interpreted to limit the scope of this invention to the specifics thereof. Rather, the scope of this invention should be evaluated with reference to the claims appended hereto. In reading the claims it is intended that when words such as "a", "an", "at least one", and "at least a portion" are used there is no intention to limit the claims to only one item unless specifically stated to the contrary in the claims. Further, when the language "at least a portion" and/or "a portion" is used, the claims may include a portion and/or the entire items unless specifically stated to the contrary. Likewise, where the term "input" or "output" is used in connection with an electric device or fluid processing unit, it should be understood to comprehend singular or plural and one or more signal channels or fluid lines as appropriate in the context. Finally, all publications, patents, and patent applications cited in this specification are herein incorporated by reference to the extent not inconsistent with the present disclosure as if each were specifically and individually indicated to be incorporated by reference and set forth in its entirety herein.

CLAIMS

The invention claimed is:

1. A nanocomposite material comprising a metal oxide bonded to a graphene layer.

2. The nanocomposite material of claim 1 wherein the graphene layer has a carbon to oxygen ratio of between 15 to 1 and 500 to1.

3. The nanocomposite material of claim 1 wherein the graphene layer has a carbon to oxygen ratio of between 20 to 1 and 500 to1.

4. The nanocomposite material of claim 1 wherein the graphene layer has a surface area of between 400 and 2630 m2/g.

5. The nanocomposite material of claim 1 wherein the graphene layer has a surface area of between 600 and 2630 m2/g.

6. The nanocomposite material of claim 1 wherein said metal oxide is M_xO_y, and where M is selected from the group consisting of Ti, Sn, Ni, Mn, V, Si, Co and combinations thereof.

7. The nanocomposite material of claim 1 wherein said metal oxide is titania.

8. The nanocomposite material of claim 1 wherein said metal oxide is tin oxide.

9. The nanocomposite material of claim 7 wherein said nanocomposite material has a specific capacity at least twice that of a titania material without the graphene layer at a charge/discharge rate greater than about 10C.

10. The nanocomposite material of claim 1 wherein said graphene layer and said metal oxides are generally uniformly distributed throughout said nanoarchitecture.

11. The nanocomposite material of claim 1 wherein said graphene layer has a thickness between 0.5 and 50 nm.

12. The nanocomposite material of claim 1 wherein the graphene layer has a thickness between 2 and 10 nm.

13. The nanocomposite material of claim 7 wherein said titania is in a mesoporous form.

14. The nanocomposite material of claim 13 wherein said mesoporous titania is in a rutile crystalline structure.

15. The nanocomposite material of claim 13 wherein said mesoporous titania is in a anatase crystalline structure.

16. A method for forming a nanocomposite material comprising the steps of:

providing graphene in a first suspension;

dispersing the graphene with a surfactant;

adding a metal oxide precursor to said dispersed graphene to form a second suspension; and

precipitating the metal oxide from the second suspension onto at least one surface of the dispersed graphene to form a nanocomposite material comprising at least one metal oxide bonded to at least one graphene layer.

17. The method as claimed in claim 16, and wherein the first suspension is, at least in part, an aqueous suspension.

18. The method as claimed in claim 16, and wherein the surfactant is an anionic surfactant.

19. The method as claimed in claim 18 and wherein the anionic sulfate surfactant is sodium dodecyl sulfate.

20. The method of claim 16 further comprising the step of heating the second suspension from 50 to 500 degrees C to condense the metal oxide on the surface of the graphene layer.

21. The method of claim 16 further comprising the step of heating the second suspension from 50 to 500 degrees C to remove the surfactant.

22. An energy storage device comprising a nanocomposite material having an active metal compound and at least one graphene layer arranged in a nanoarchitecture.

23. The nanocomposite material of claim 22 wherein the graphene layer has a carbon to oxygen ratio between 15 to 1 and 500 to 1.

24. The nanocomposite material of claim 22 wherein the graphene layer has a carbon to oxygen ratio of between 20 to 1 and 500 to 1.

25. The nanocomposite material of claim 23 wherein the graphene layer has a surface area of between 400 and 2630 m^2/g.

26. The nanocomposite material of claim 23 wherein the graphene layer has a surface area of between 600 and 2630 m^2/g.

27. The energy storage device of claim 25, wherein said nanocomposite material has a specific capacity at least twice that of a titania material without graphene at a charge/discharge rate greater than about 10C.

28. The energy storage device of claim 27 wherein said graphene layer and said metal oxide are generally uniformly distributed throughout said nanoarchitecture.

29. The energy storage device as claimed in claim 28 and wherein the energy storage device is an electrochemical device having an anode, a cathode, an electrolyte, and a current collector.

30. The energy storage device as claimed in claim 29, and wherein at least one of the anode, cathode, electrolyte, and current collector is fabricated from, at least in part, the nanocomposite material.

31. The energy storage device as claimed in claim 29, and wherein the anode is fabricated from, at least in part, the nanocomposite material, and wherein the anode contains less than 10% graphene material by weight.

32. The energy storage device as claimed in claim 29 and wherein the anode is fabricated from, at least in part, the nanocomposite material, and wherein the anode contains less than 5% graphene material by weight.

33. The energy storage device as claimed in claim 29, and wherein the cathode is fabricated from, at least in part, the nanocomposite material, and wherein the cathode contains less than 5% graphene material by weight.

34. The energy storage device as claimed in claim 29, and wherein the cathode is fabricated from, at least in part, the nanocomposite material,

and wherein the cathode contains less than 2.5% graphene material by weight.

35. The energy storage device as claimed in claim 29, and wherein the electrochemical device is a lithium ion battery.

36. A lithium ion battery electrode comprising at least one graphene layer bonded to titania to form a nanocomposite material, and wherein the graphene layer has a carbon to oxygen ration of between 15 to 1 and 500 to 1 and a surface area of between 400 and 2630 m^2/g, and wherein said nanocomposite material has a specific capacity at least twice that of a titania material without graphene material at a charge/discharge rate greater than about 10C.

37. The lithium ion battery electrode as claimed in claim 36, and further comprising multiple nanocomposite material layers uniformly distributed throughout the electrode.

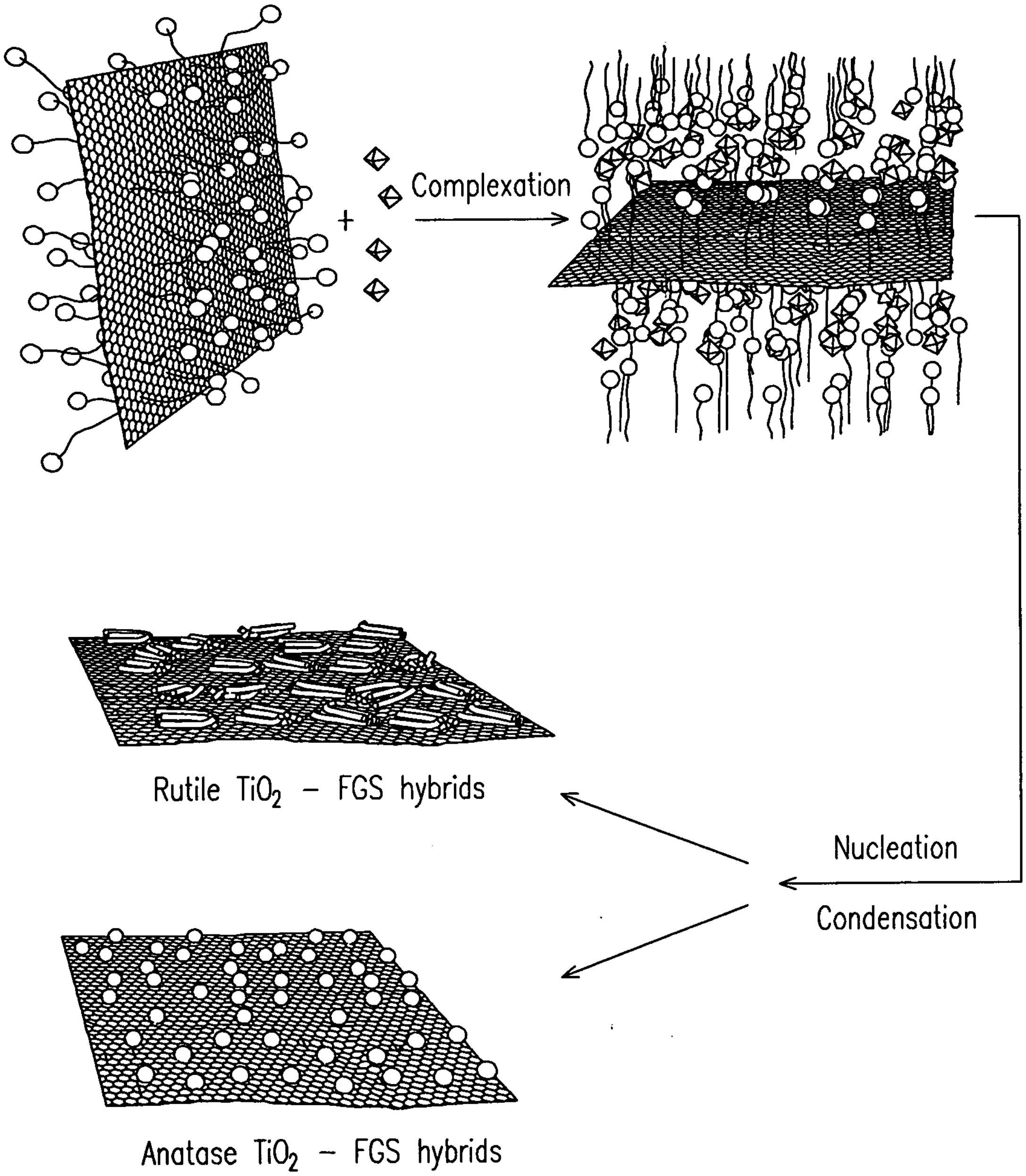
+
Complexation
Rutile TiO_2 – FGS hybrids
Nucleation
Condensation
Anatase TiO_2 – FGS hybrids

Fig. 1

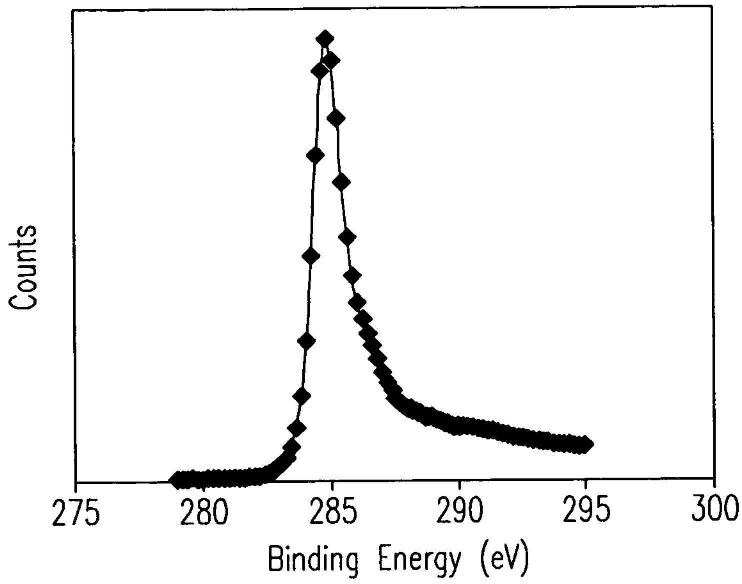
Counts
275
280
285
290
295
300
Binding Energy (eV)

Fig. 2

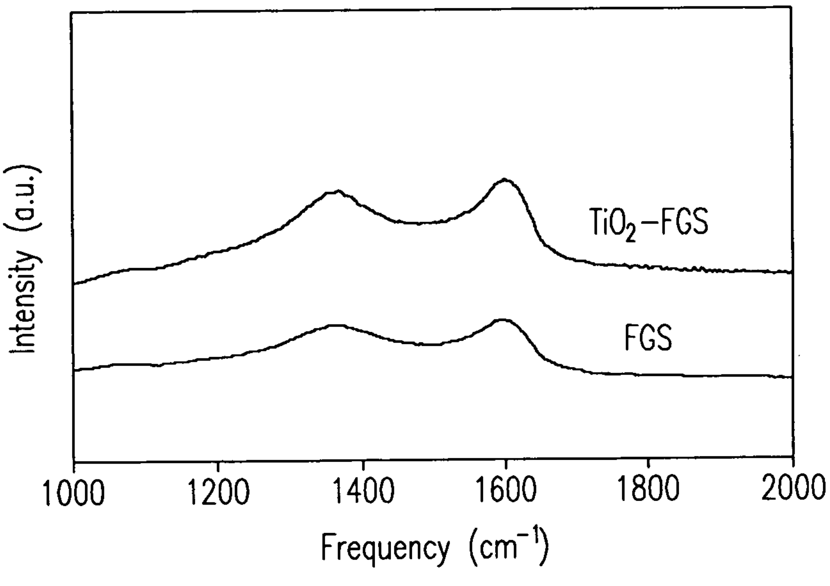
Intensity (a.u.)
TiO_2-FGS
FGS
1000
1200
1400
1600
1800
2000
Frequency (cm^{-1})

Fig. 3

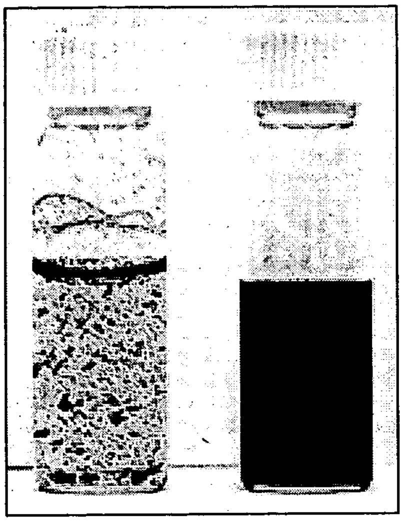

Fig. 4a

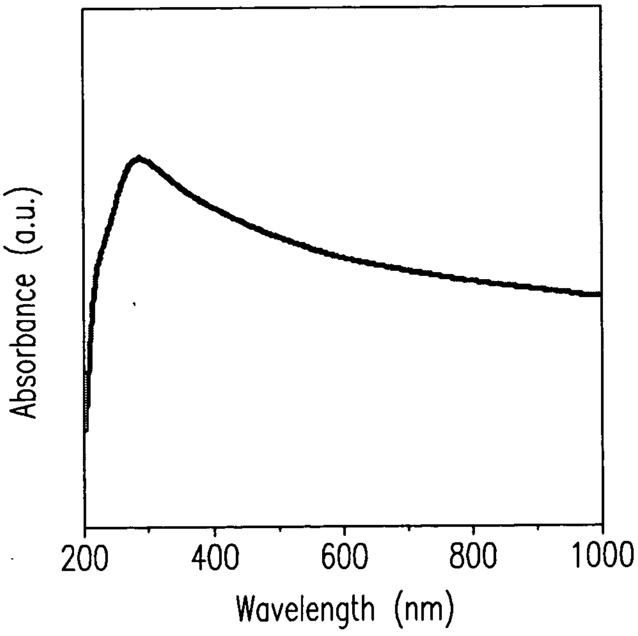

Fig. 4b

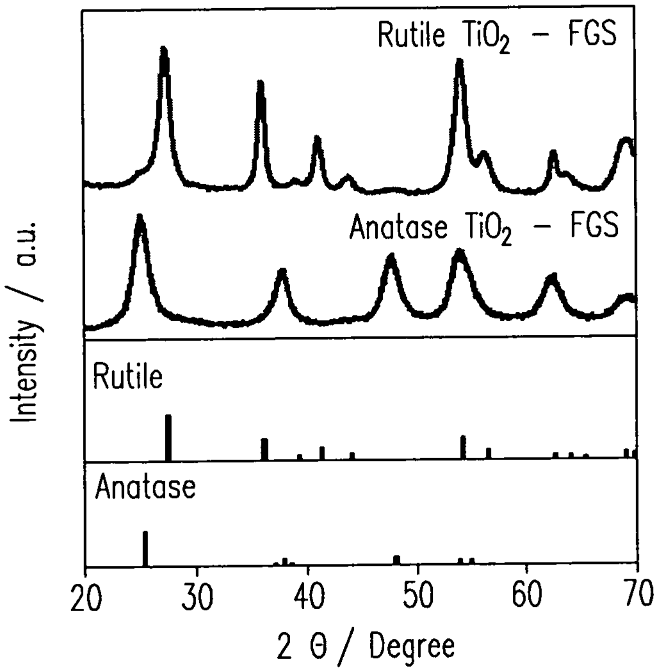

Fig. 5

Fig. 6a

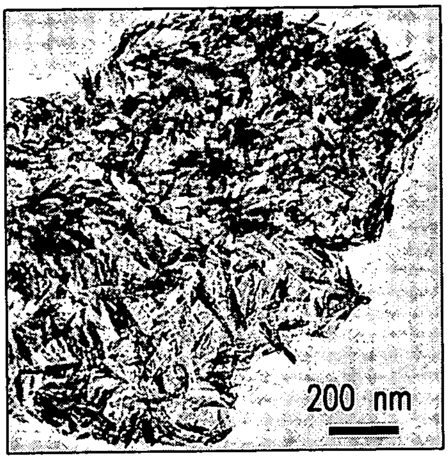

Fig. 6b

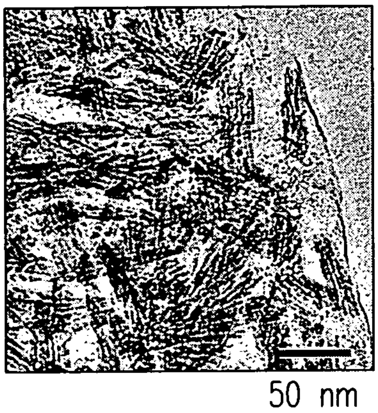

Fig. 6c

Fig. 6d

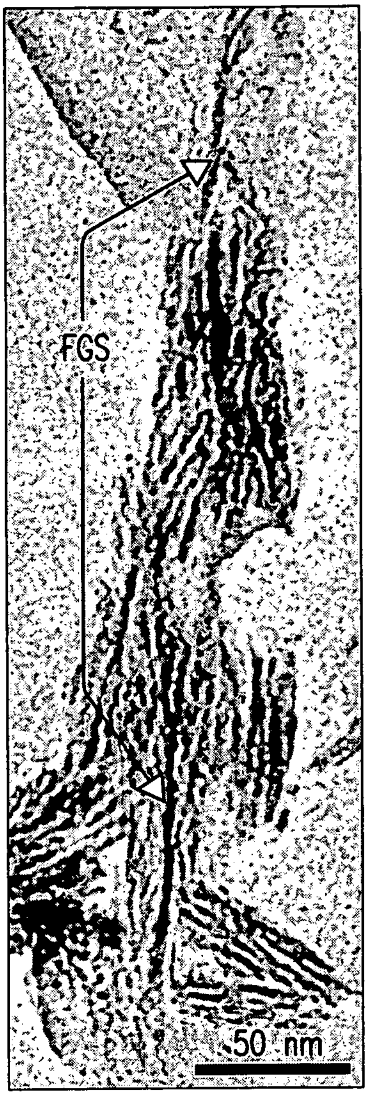

Fig. 6e

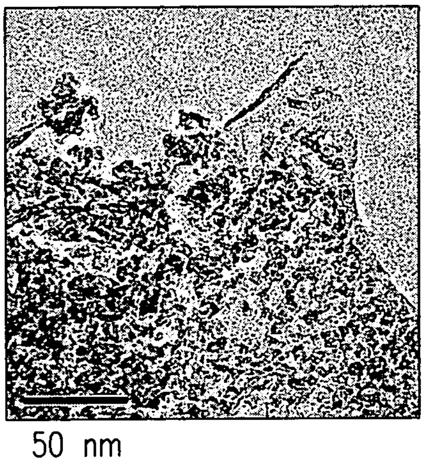

Fig. 6f

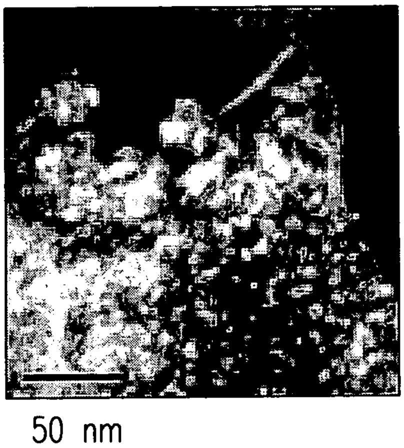

Fig. 6g

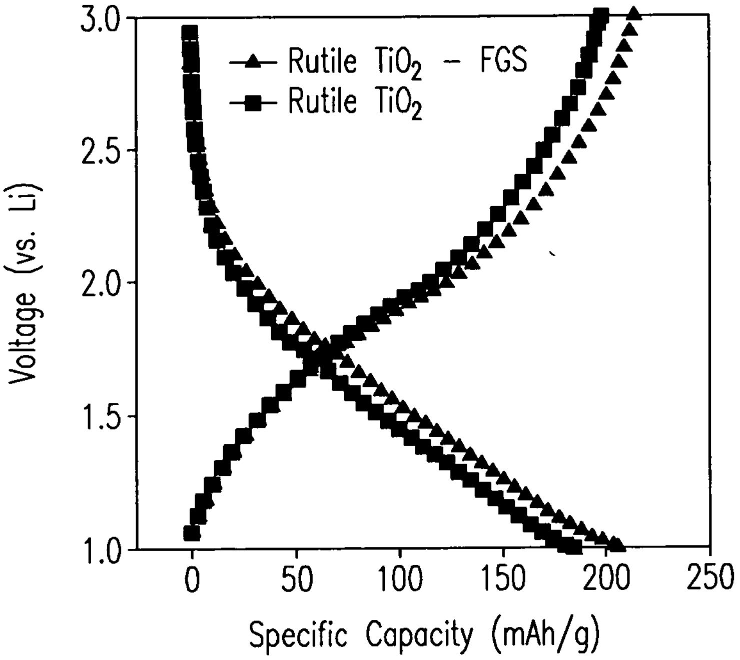
Voltage (vs. Li)
3.0
2.5
2.0
1.5
1.0
0
50
100
150
200
250
Specific Capacity (mAh/g)
Rutile TiO_2 - FGS
Rutile TiO_2

Fig. 7a

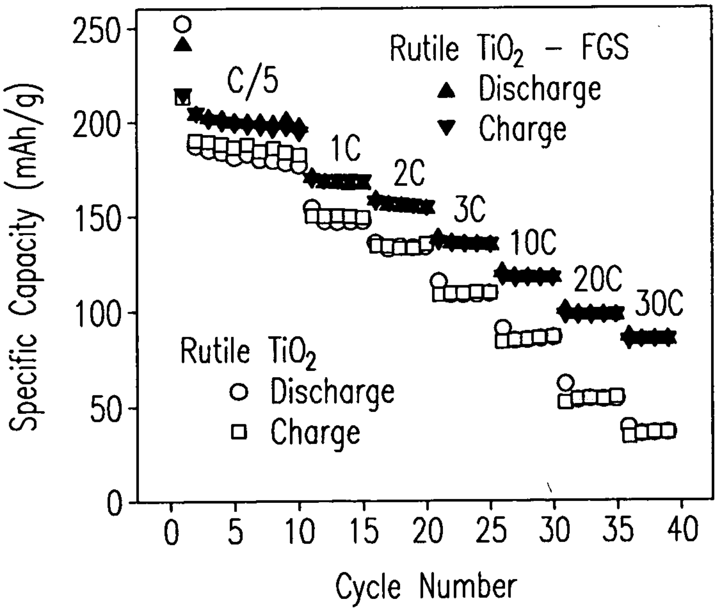
Specific Capacity (mAh/g)
250
200
150
100
50
0
0
5
10
15
20
25
30
35
40
Cycle Number
C/5
1C
2C
3C
10C
20C
30C
Rutile TiO_2 - FGS
▲ Discharge
▼ Charge
Rutile TiO_2
○ Discharge
□ Charge

Fig. 7b

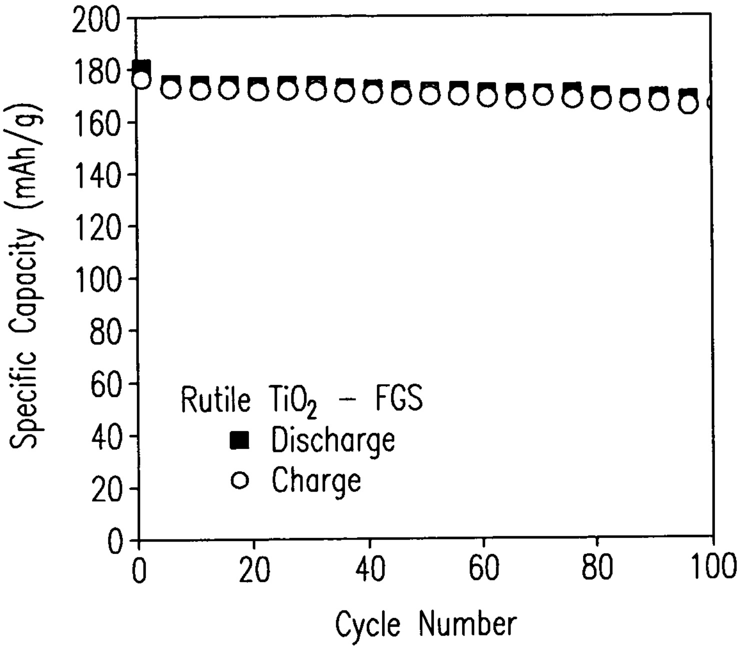
Specific Capacity (mAh/g)
200
180
160
140
120
100
80
60
40
20
0
Rutile TiO_2 - FGS
■ Discharge
○ Charge
0
20
40
60
80
100
Cycle Number

Fig. 7c

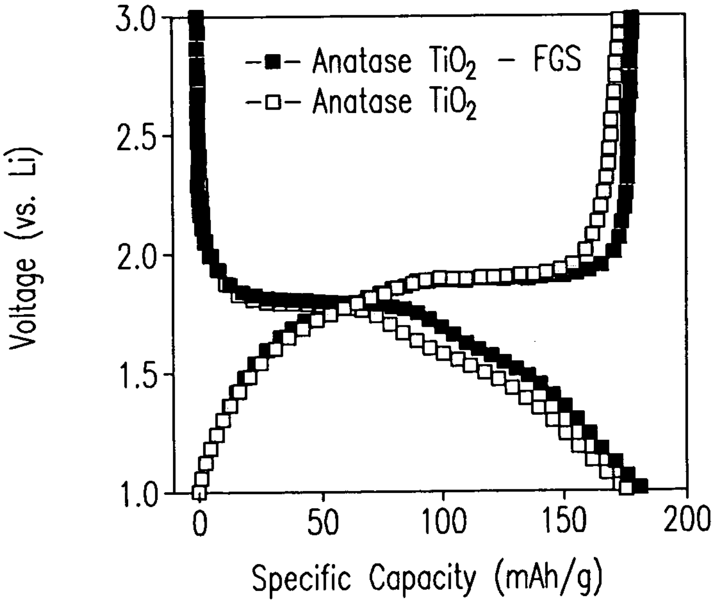
Voltage (vs. Li)
3.0
2.5
2.0
1.5
1.0
-■- Anatase TiO_2 - FGS
-□- Anatase TiO_2
0
50
100
150
200
Specific Capacity (mAh/g)

Fig. 7d

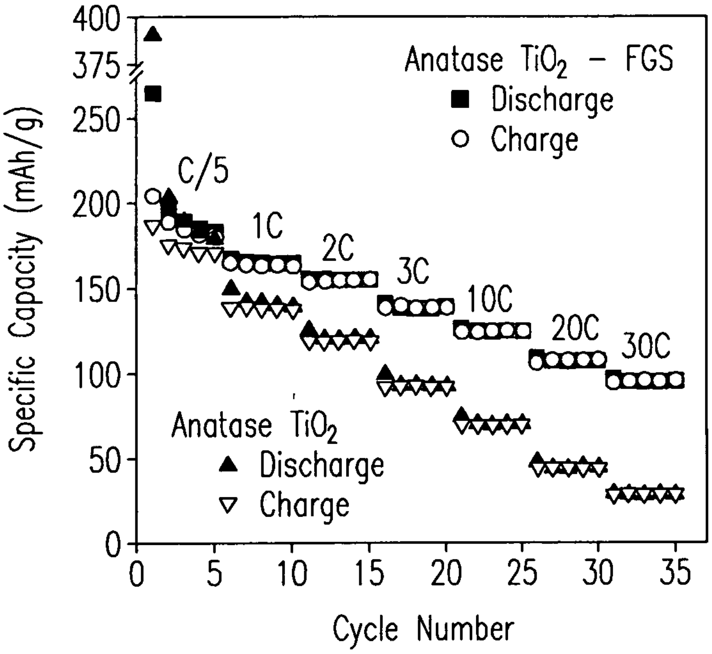

Specific Capacity (mAh/g)
400
375
250
200
150
100
50
0
0
5
10
15
20
25
30
35
Cycle Number
Anatase TiO₂ - FGS
■ Discharge
○ Charge
C/5
1C
2C
3C
10C
20C
30C
Anatase TiO₂
▲ Discharge
▽ Charge

Fig. 7e

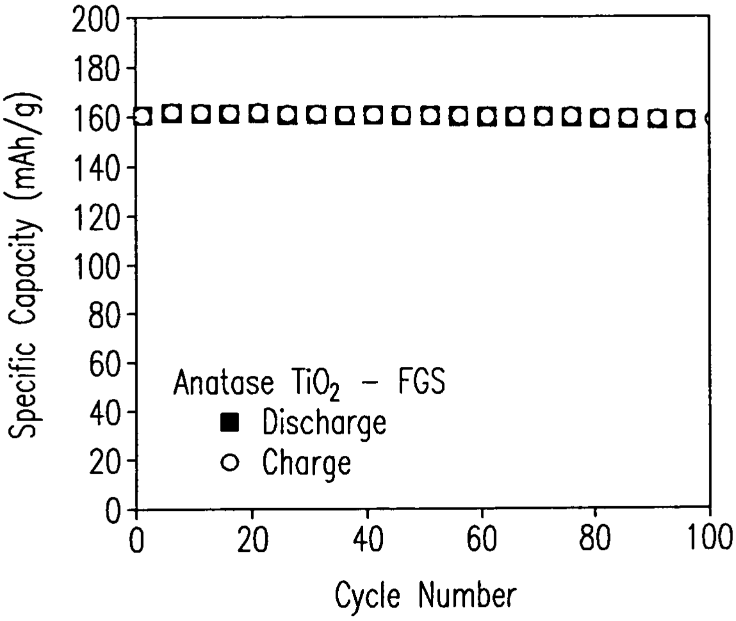

Specific Capacity (mAh/g)
200
180
160
140
120
100
80
60
40
20
0
0
20
40
60
80
100
Cycle Number
Anatase TiO₂ - FGS
■ Discharge
○ Charge

Fig. 7f

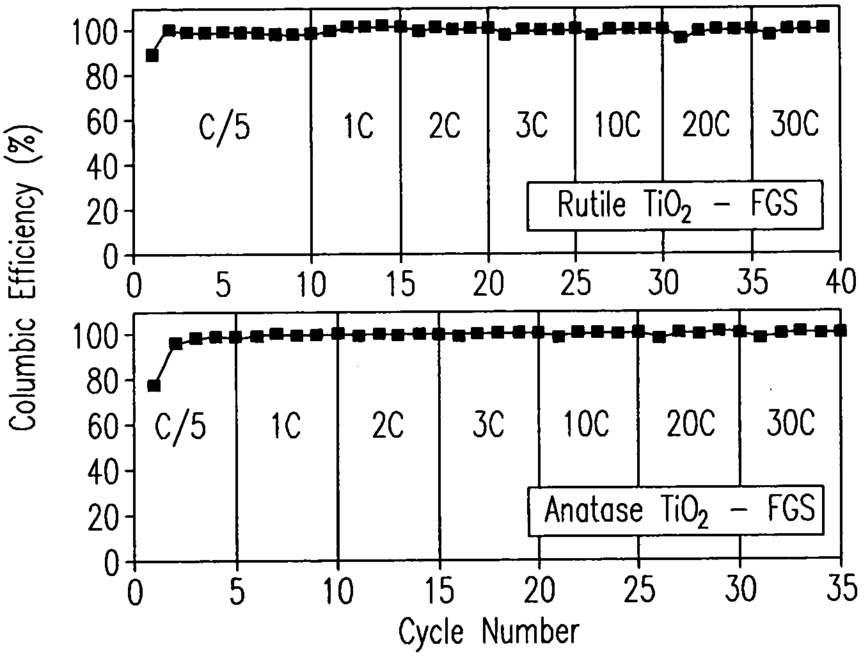
Columbic Efficiency (%)
100
80
60
40
20
0
C/5
1C
2C
3C
10C
20C
30C
Rutile TiO_2 – FGS
0
5
10
15
20
25
30
35
40
Anatase TiO_2 – FGS
0
5
10
15
20
25
30
35
Cycle Number

Fig. 8

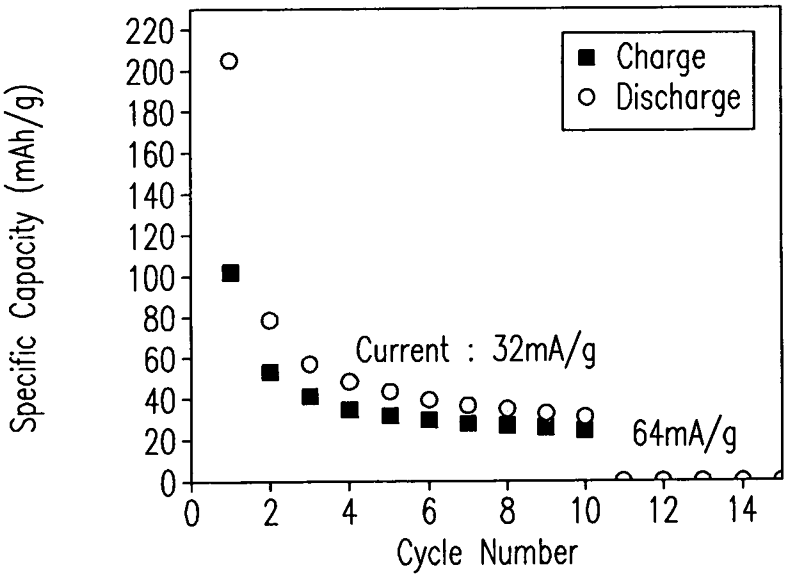
Specific Capacity (mAh/g)
220
200
180
160
140
120
100
80
60
40
20
0
■ Charge
○ Discharge
Current : 32mA/g
64mA/g
0
2
4
6
8
10
12
14
Cycle Number

Fig. 9

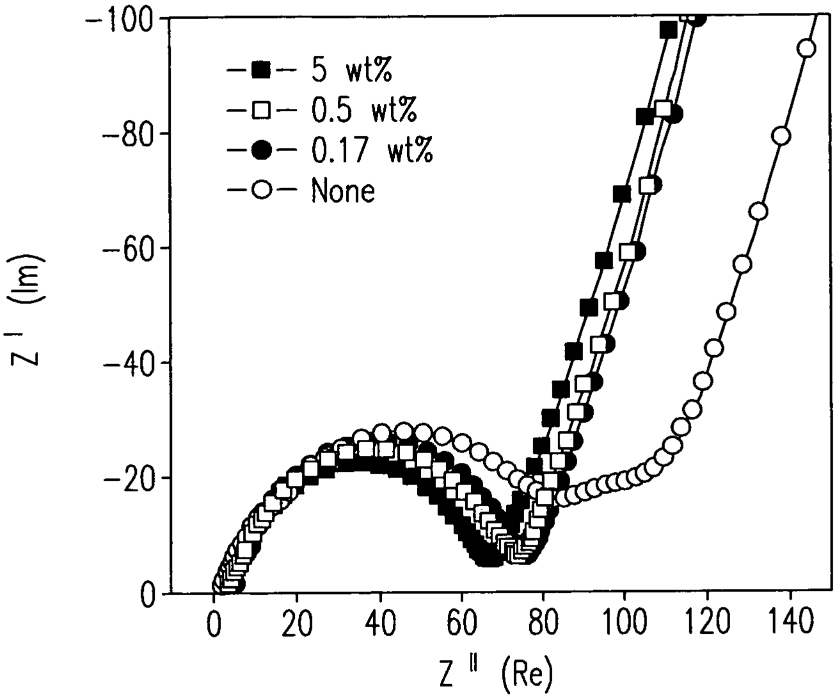

Fig. 10a

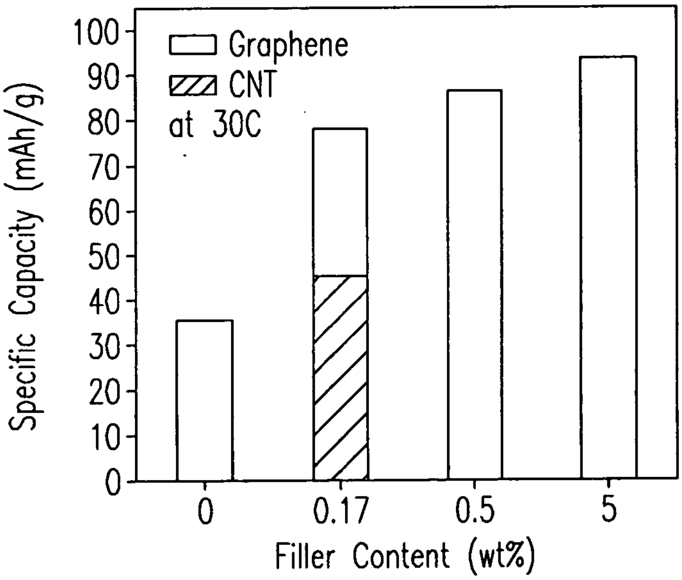

Fig. 10b

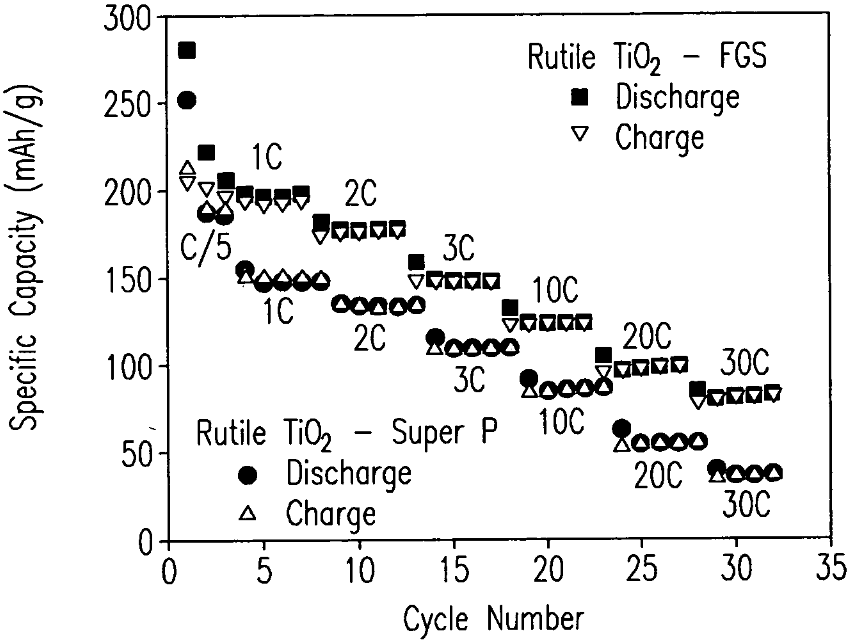

Specific Capacity (mAh/g)
0
50
100
150
200
250
300
0
5
10
15
20
25
30
35
Cycle Number
Rutile TiO_2 - FGS
■ Discharge
▽ Charge
Rutile TiO_2 - Super P
● Discharge
△ Charge
C/5
1C
2C
3C
10C
20C
30C
1C
2C
3C
10C
20C
30C

Fig. 11

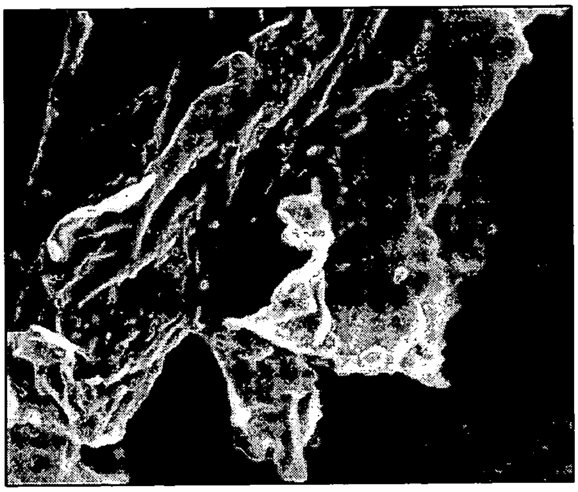

Fig. 12